JOURNAL OF SOLID STATE CHEMISTRY **132,** 411–419 (1997)
ARTICLE NO. SC977499

Structural and Nonlinear Optical Characterizations of Tellurium Oxide-Based Glasses: TeO_2–BaO–TiO_2

J. C. Sabadel,* P. Armand,* D. Cachau-Herreillat,* P. Baldeck,† O. Doclot,† A. Ibanez,†† and E. Philippot*

** LPMC, UMR 5617 CNRS, UMII, place E. Bataillon, C.C.003, 34095 Montpellier Cedex 5, France; and † LSP, UMR 5588 CNRS, Université J. Fourier, B.P. 87, 38402 St. Martin d'Heres Cedex, France; and †† Laboratoire de Cristallographie, CNRS, UPR 5031, BP 166, 38042 Grenoble Cedex 09, France*

Received January 16, 1997; in revised form May 27, 1997; accepted May 28, 1997

The structure of the pseudo ternary TeO_2–TiO_2–BaO glasses was investigated by Raman and infrared spectroscopies. In the TeO_2–BaO system, glasses with low BaO content have a continuous network constructed by sharing corners of TeO_4 trigonal bipyramids and TeO_{3+1} polyhedra having nonbridging oxygen atoms. In glasses containing 40% mol BaO, isolated structural units such as TeO_3 are formed. However, TiO_2 insertion can inhibit this structural change and favor a continuous network. We discuss the characterization of nonlinear optical process in these materials using Z scan technique. The highest nonlinear absorption values are obtained for titanium tellurite glasses emphasising the particularly significant role of the structural units in the optical response.

INTRODUCTION

Because of their high infrared transmission, high refractive index and low dispersion (1–3), tellurite glasses are of considerable interest for various optical devices.

TeO_2-based glasses also possess physical properties which are not only interesting from the fundamental point of view but are important for practical applications using nonlinear optical properties, such as optical modulators and memories (4). Much attention has been focused on glassy materials because of their large optical nonlinearity and their fast response time in bulk or fibre waveguide form with high optical quality.

The ability to tailor the nonlinear effect of glass has been used in such diverse applications as controlling beam breakup in high power lasers and optical devices for switching and logic. Some recent works (5, 6), based on infrared and Raman scattering studies, confirmed that TeO_2-based glasses with low modifier content are formed by a three-dimensional network composed of TeO_4 trigonal bipyramids (tbp's). Binary TeO_2 glasses containing alkaline oxides as network modifiers change their structure from TeO_4 to TeO_{3+1} and then to TeO_3 units when the modifier content increases (7).

The present work started with the purpose of examining the structure of the BaO–TeO_2–TiO_2 glasses and of establishing a relation between structure and nonlinear optical characteristics. We measured the optical nonlinearities of the TeO_2–BaO–TiO_2 system using the Z scan method (8). Moreover, infrared and Raman investigations of tellurite glasses and their crystalline analogues show that the position and the intensity of the bands for Te–O stretching vibrations characterize Te–O polyhedra (9–11). The introduction of other elements such as Ba or Ti changes the coordination of Te atoms in the glasses and may also affect physical properties of the glasses.

EXPERIMENTAL

Glass samples were prepared by using reagent grade, TeO_2 (99.995% Aldrich), $BaCO_3$ (99.9% Merck), and TiO_2 anatase (99.9 + Aldrich) as starting materials. Samples were weighed in 2–5 g batches and mixed thoroughly in an agate mortar. The mixture was then heated in a gold or platinum crucible placed in an electric furnace at 650°C for 4 hours, with a heating rate of 5°C/min, to drive off CO_2. The resultant mixture was melted for about 2 hours at 900–950°C, depending on composition. A specific experimental mechanism makes it possible to homogenize the resultant liquid during the heating. The liquid thus obtained was poured into a stainless steel mold initially preheated at 200°C to decrease failures due to mechanical stress into the glass.

The fast roller quenching technique was used to extend the glass forming region. Figure 1 shows the limits of the vitreous domains in the TeO_2–BaO–TiO_2 system according to the two quenching techniques. Amorphous state of the samples was checked by X-ray diffraction (using Cu$K\alpha$ radiation) and the glassy state confirmed by differential scanning calorimetry (DSC) studies.

0022-4596/97 $25.00

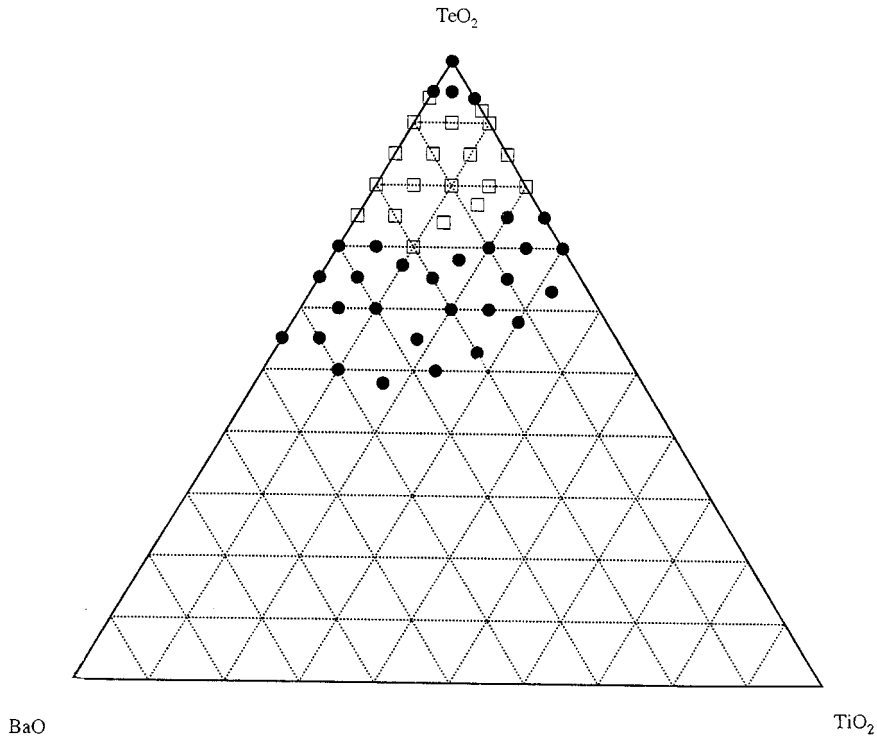

FIG. 1. Glass-forming region: (□) glasses obtained by the classic technique, (●) glasses obtained by the roller technique.

Infrared measurements were carried out using a BOMEM DA8 spectrometer in the wave number range 400–4000 cm^{-1} by the KBr pellet method and Raman spectra were recorded in the range 50–1200 cm^{-1} with an OMARS 89 of Dilor society Raman spectrophotometer (the wave number accuracy of all sharp bands is $\pm 4\ cm^{-1}$ for the two spectroscopies). The sample, previously polished in a 2.2.1 mm^3 bulk, was excited with an argon ionized laser (Spectra Physics 2020 series) at 514.5 nm with a power between 10 and 100 mW, and the spectrum was observed at an angle of 90° to the exciting light.

Z SCAN EXPERIMENTAL

In the Z scan technique, the sample is moved along the z direction and very small effects are recorded. For this reason, very high sample quality is required. The third-order nonlinearities of a TeO_2–TiO_2–BaO glasses series have been measured using the single beam method called Z scan (12).

A scheme of the Z scan experimental setup is shown in Fig. 2. The transmittance (D_1/D_2) of a tightly focused Gaussian beam through a finite aperture S (linear transmission)

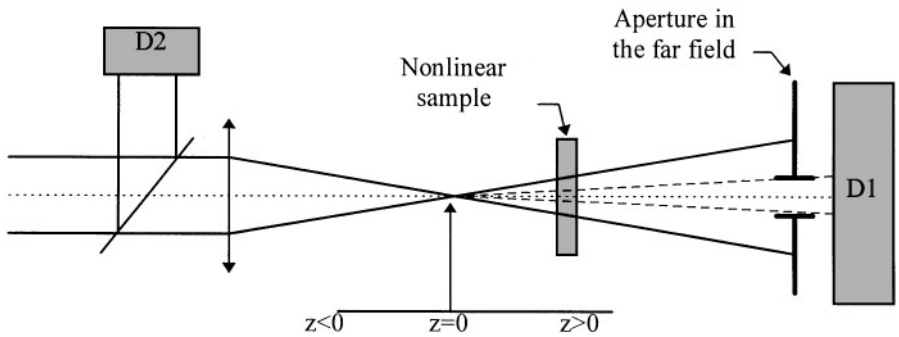

FIG. 2. Scheme of the Z scan experimental setup.

in the far field is measured as a function of the sample position z with respect to the focal plane. At each position, the sample experiences a different incident field (i.e., amplitude and phase). Nonlinear refraction in the sample causes beam broadening or narrowing in the far field and thus modifies the fraction of light passing through the aperture as the sample position is changed. In the case of a material with a positive nonlinear refractive index, the beam broadening (narrowing) in the far field occurs when the sample is situated before (after) the focus. A decrease in transmittance followed by an increase of transmittance (valley–peak) for increasing z then denotes a positive nonlinear refraction, while a peak–valley configuration characterizes a negative nonlinearity.

As far as the sample can be considered as thin compared to the beam Rayleigh range z_0, the difference in transmittance between the peak and the valley $\Delta T_{p,v}$ is simply related to the nonlinear refractive index n_2 (13)

$$\Delta T_{p,v} = 0.406(1 - S)^{0.25} \cdot \frac{2\pi}{\lambda} \cdot \frac{n_2}{\sqrt{2}} \cdot I_0 \cdot L_{\text{eff}}, \qquad [1]$$

where n_2 is expressed in meters^2 per watts and $n = n_0 + n_2 I$, I_0 is the peak-on-axis irradiance at focus expressed in watts per meter^2 inside the sample, λ is the wavelength expressed in meters, $L_{\text{eff}} = (1 - e^{-\alpha_0 L})/\alpha_0$ is the effective length and α_0 is the linear absorption of the sample, and $1/\sqrt{2}$ is a time average factor used for temporally Gaussian pulses having pulsewidth longer than the nonlinearity response time.

Removing the aperture in the far field enables nonlinear absorption measurements since a Z scan with a fully opened aperture ($S = 1$) is insensitive to nonlinear refraction. Such Z scan traces are expected to be symmetric with respect to the focus ($z = 0$) where they exhibit a minimum transmittance in the case of nonlinear absorption (e.g., multiphoton absorption). In this case the normalized energy transmittance is given by (13)

$$T_{\text{norm}}(Z) = \frac{1}{\sqrt{\pi}} \cdot \frac{1}{q_0(z,0)} \cdot \int \ln(1 + q_0(z,0) \cdot \exp(-t^2))dt, \qquad [2]$$

where

$$q_0(z,t) = \frac{\beta \cdot L_{\text{eff}} \cdot I_0(t)}{I + (z/z_0)^2}.$$

β is the nonlinear absorption coefficient expressed in meters per watt or more commonly in centimeters per gigawatt with $\alpha = \alpha_0 + \beta \cdot I_0$ representing the sample absorption expressed in centimeters^{-1}.

When the aperture is in place, the measurement is sensitive to both nonlinear refraction and absorption. Dividing the closed aperture data by the open aperture data yields a Z scan signal typical of a purely refractive nonlinearity.

In this paper, we report measurements performed at 532 nm with a frequency-doubled single pulse extracted from a mode-locked and Q-switched Nd:Yag laser by a Pockels cell. The laser operated in the TEM_{00} mode at a 60-Hz repetition rate. The temporal width of the pulses was 250 ps (FWHM). The laser parameters (waist, I_0) were calibrated thanks to a 1-mm cell filled with CS_2, the nonlinear refractive index of which is known to be equal to $n_2(CS_2) = (3.1 \pm 0.5) \times 10^{-18}$ m^2 W^{-1} (13).

As I_0 represents the intensity inside the sample, all the intensities given by the CS_2 calibration were corrected by the interfaces reflectivities.

STRUCTURAL CHARACTERIZATIONS

Raman Study

To interpret the Raman spectra of glass materials, one of the best ways is to compare them to those of crystallized references with comparable composition. For this reason, we have first undertaken the investigation of Raman spectra of the crystallized materials: αTeO_2, rutile and anatase TiO_2, $BaTeO_3$, Ba_2TiO_4, and $TiTe_3O_8$.

The structural unit of αTeO_2 can be described as a trigonal bipyramid (tbp) commonly called TeO_4E, where one of the three equatorial directions is occupied by the $5s^2$ electronic lone pair (E) of the tellurium atom with the two equatorial distances (2×1.91 Å) shorter than the two axial distances (2×2.09 Å). The environment of these Te atoms is completed by two other longer and equatorial interactions (≈ 2.9 Å) and the three-dimensional close packing is built up from vertice sharing TeO_4 groups (Te–$_{eq}$O$_{ax}$–Te) reinforced by weaker Te–O interactions ($d_{Te-O} \approx 2.9$ Å) (14).

The Raman spectrum of αTeO_2 is given in Fig. 3a. The peak at 650 cm^{-1} is assigned to $\nu_{s1}TeO_4$: two equatorial and two axial bonds stretch in the same phase (15). Around 590 cm^{-1}, two equatorial bonds stretch in the reverse phase and two bonds vibrate in the same manner: it is assigned to $\nu_{as}TeO_4$. The peak around 400 cm^{-1} is assigned to symmetric stretching vibrations of Te–$_{eq}$O$_{ax}$–Te.

Figure 3b shows the spectrum of monoclinic $BaTeO_3$ which has the usual trigonal pyramidal shape called TeO_3E with the lone pair E, opposite to the basal plane ($2 \times d_{Te-O} = 1.86$ Å and $d_{Te-O} = 1.88$ Å) (16).

Rutile and anatase TiO_2 structures are both tetragonal: each Ti atom is coordinated to six O atoms and each O atom is coordinated to three Ti atoms. In each case, the TiO_6 octahedron is slightly distorted, with two Ti–O axial bonds greater than the other four and with some O–Ti–O bond angles deviating from 90°, see Table 1. These structures have been described in terms of chains of TiO_6 octahedra having common edges (17), but the distortion is

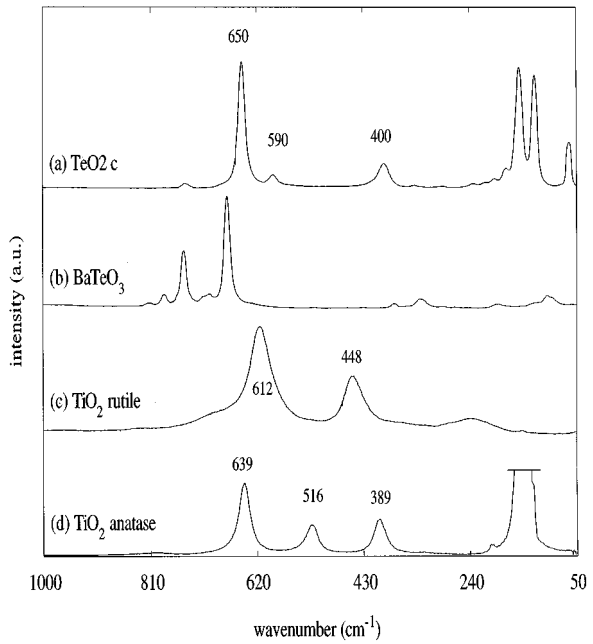

FIG. 3. Raman spectra of (a) α-TeO_2, (b) $BaTeO_3$, (c) rutile TiO_2, and (d) anatase TiO_2.

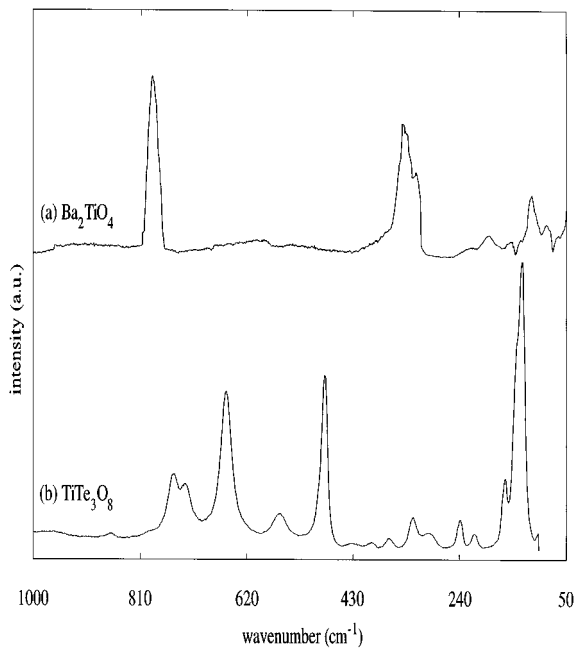

FIG. 4. Raman spectra of (a) β-Ba_2TiO_4 and (b) $TiTe_3O_8$ crystallized phases.

greater in anatase than in rutile. The spectra are presented in Figs. 3c and 3d.

βBa_2TiO_4 is one of the rare titanates where the structure is characterized by titanium atoms in tetrahedral coordination. The Ti atom is surrounded by a distorted tetrahedron of oxygen atoms and the structure may be also regarded as a sequence of TiO_4 groups (18–20). Its spectrum is given in Fig. 4a.

In $TiTe_3O_8$, Fig. 4b, the tellurium atom environment is slightly more distorted than that in αTeO_2 (two equatorial Te–O bonds shorter and two axial bonds longer), and the titanium atoms are sixfold coordinated as in TiO_2 (21).

By comparison with the Raman spectra of crystalline compounds, the local environment of the different atoms in tellurium oxide-based glasses can be approached. Raman spectrum of pure TeO_2 glass is shown in Fig. 5. Sekiya *et al.* (15) have deconvoluted the spectrum into symmetric Gaussian functions with five peaks which agree with the frequencies of paratellurite. TeO_2 glass structure is essentially based on that of αTeO_2 consisting of TeO_4 tbp units. The shoulder at 750 cm^{-1}, as encountered in $BaTeO_3$, can be due to a more distorted TeO_4 groups than in αTeO_2. This result is in accordance with the evolution observed in the pseudo binary $(1-x)TeO_2 - xBaO$ system (Fig. 5). When the BaO

TABLE 1
Interatomic Distances and Angles for Rutile and Anatase TiO_2

	d_{Ti-O} (Å)	O–Ti–O (°)	O–Ti–O (°)	O–Ti–O′ (°)	Ti–O–Ti (°)
TiO_2 rutile	4 × 1.9486	2 × 98.79	2 × 180	4 × 90	2 × 130.60
	2 × 1.9796	2 × 81.21		4 × 90	1 × 98.79
TiO_2 anatase	4 × 1.9338	2 × 92.43	2 × 156.23	4 × 78.12	2 × 101.88
	2 × 1.9799	2 × 92.43		4 × 101.88	1 × 156.23

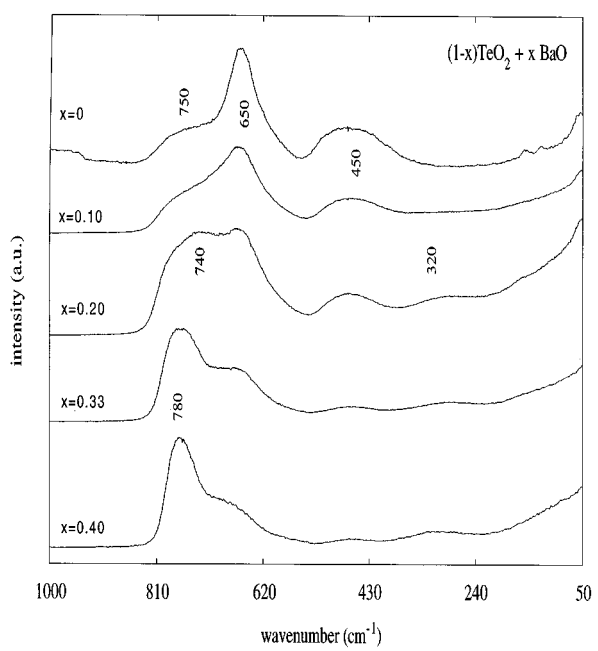

FIG. 5. Intensity-normalized Raman spectra of the $(1-x)TeO_2 + xBaO$ glasses.

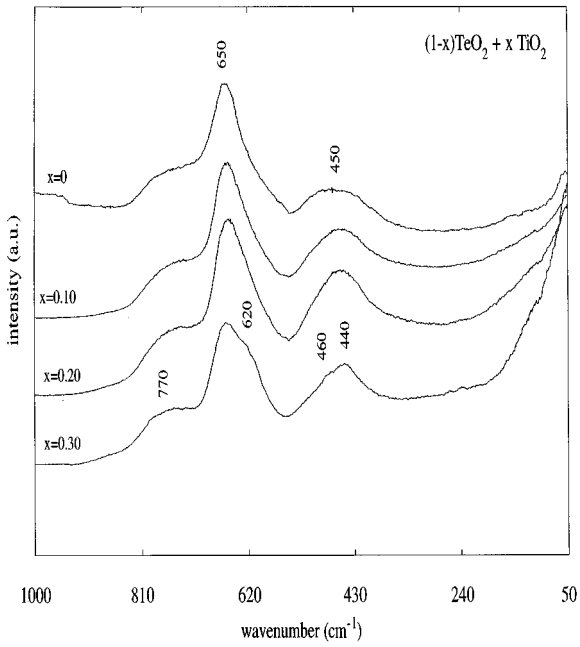

FIG. 6. Intensity-normalized Raman spectra of the $(1-x)TeO_2 + xTiO_2$ glasses.

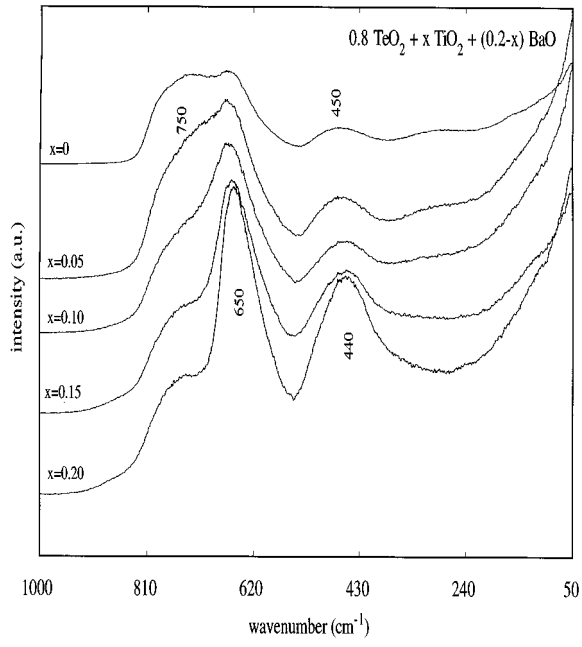

FIG. 7. Intensity-normalized Raman spectra of the $0.8TeO_2 + (0.2-x)BaO + xTiO_2$ glasses.

content increases, the large characteristic band of TeO_4 units at 650 cm^{-1} vanishes to the benefit of the one of TeO_3 entities at 780 cm^{-1} (22). The coordination of the Te atom changes progressively from 4 to 3 through 3+1 (band at 740 cm^{-1} for $x = 0.22$ and $x = 0.33$) where one Te–O_{ax} distance is elongated while the opposite is shortened: then this TeO_{3+1} asymmetric polyhedron possesses three short Te–O distances between 1.85 and 2 Å and one greater than 2.25 Å. The weak broadband about 320 cm^{-1} observed for $x \geq 0.10$ is assigned to the bending vibrations of TeO_3 tp's with nonbridging oxygen (NBO) atoms (23).

The spectra of $(1-x)TeO_2 + xTiO_2$ ($0 \leq x \leq 0.3$) glasses are presented in Fig. 6. For this pseudo binary system, the increase of TiO_2 content does not strongly modify the characteristic band of TeO_4 groups at 650 cm^{-1}. On the other hand, the increase of the large diffusion band centered at 440 cm^{-1} is due to the distorted octahedral environment of Ti atoms like in TiO_2 rutile and $TiTe_3O_8$ (Fig. 4b) which corresponds to the $0.75TeO_2 + 0.25TiO_2$ composition. Then, in these glasses, the titanium atoms do not exhibit a tetrahedral coordination as in βBa_2TiO_4.

Finally, if we consider the pseudo ternary system with a fixed TeO_2 concentration: $0.8TeO_2 + xTiO_2 + (0.2-x)BaO$ with $0 \leq x \leq 0.2$ (Fig. 7), we observe a reinforcement of the absorption band at 650 cm^{-1} and, in parallel, a decrease of that at 750 cm^{-1}, clearly indicating that the coordination of tellurium atoms becomes again 4 when the TiO_2 content increases.

In conclusion of this Raman study, the tellurium coordination seems slightly more distorted in TeO_2 glass than in αTeO_2. This coordination decreases with the BaO content but stays approximately the same with the TiO_2 content. On the other hand, the titanium atoms are always in distorted octahedral sites, whatever their concentration.

In order to complete this Raman structural approach, we have undertaken an investigation by infrared spectroscopy.

Infrared Study

According to Dimitriev *et al.* (24), the infrared (IR) frequencies of αTeO_2 (Fig. 8b) considered with a C_{2v} symmetry, are assigned as follows:

$$\nu_1(A1) = \nu_s TeO_{2eq} = 780\ cm^{-1}\ \text{(sharp)},$$

$$\nu_8(B1) = \nu_{as} TeO_{2eq} = 714\ cm^{-1}\ \text{(shoulder)},$$

$$\nu_6(B_2) = \nu_{as} TeO_{2ax} = 675\ cm^{-1}\ \text{(broad)},$$

$$\nu_2(A1) = \nu_s TeO_{2ax} = 635\ cm^{-1}\ \text{(shoulder)}.$$

In the same way, two absorption bands are observed in the IR spectra of crystalline tellurites built up from TeO_3 groups, as in $BaTeO_3$ (Fig. 8a): $\nu_s TeO_3 = 750\ cm^{-1}$ and $\nu_d TeO_3 = 680\ cm^{-1}$.

The infrared spectrum of βBa_2TiO_4 (Fig. 9a) shows only one diffuse band centered at 700 cm^{-1}, characterizing the TiO_4 units. The spectrum of $TiTe_3O_8$ (Fig. 9b) shows four

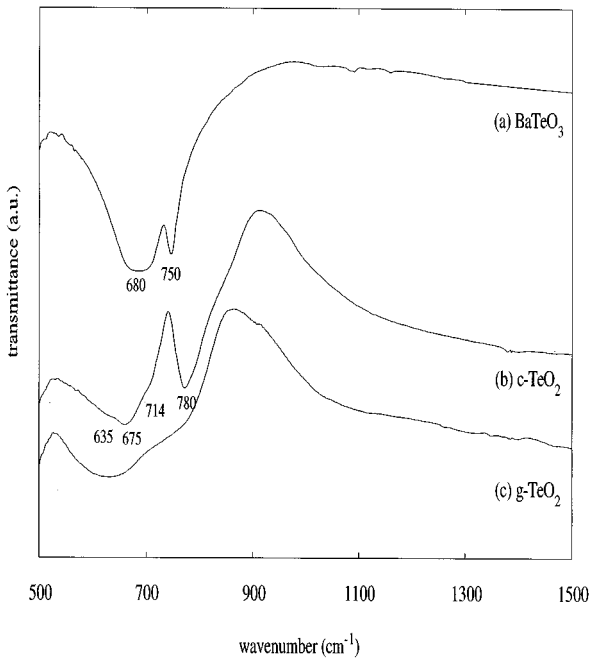

FIG. 8. Infrared spectra of (a) $BaTeO_3$, (b) α-TeO_2, and (c) pure TeO_2 glass.

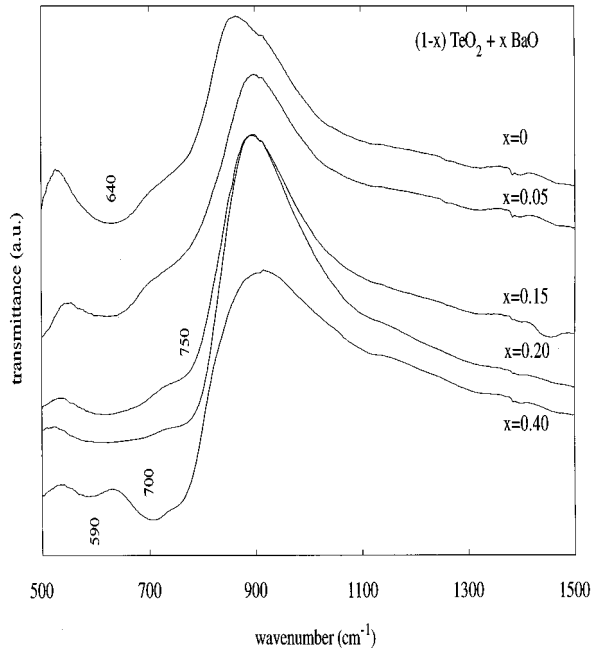

FIG. 10. Infrared spectra of the $(1-x)TeO_2 + xBaO$ glasses.

sharp absorption bands in the range 570–760 cm^{-1}, due to TeO_4 and TiO_6 entities.

Now, if we compare these infrared spectra of crystallized powders with those recorded for the glasses, the tetracoordination of tellurium atoms in pure TeO_2 glass can be confirmed. In this case, only one large and diffuse band is observed which is the envelope of both sharp bands at 675 and 780 cm^{-1} for αTeO_2, as illustrated in Fig. 8, which is explained by a decrease of symmetry of the TeO_4 polyhedra.

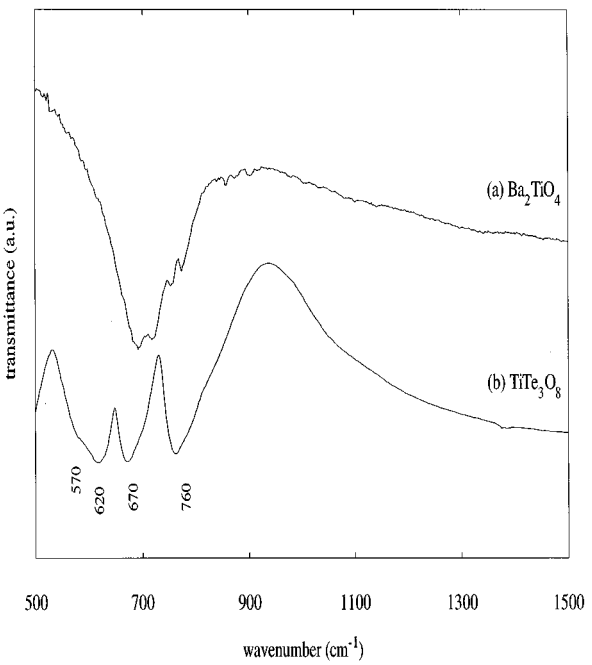

FIG. 9. Infrared spectra of (a) β-Ba_2TiO_4 and (b) $TiTe_3O_8$ crystallized compounds.

Spectra of $(1-x)TeO_2 + xBaO$ glasses ($0 \leq x \leq 0.4$) are presented in Fig. 10. When the modifier BaO is added to TeO_2, the broadband at 640 cm^{-1} decreases and shifts to lower frequencies around 590 cm^{-1}. On the other hand, the shoulder at 750 cm^{-1} becomes more pronounced with the appearance of a band at 700 cm^{-1}. This large band is the envelope of the two characteristic bands of $BaTeO_3$ (680 and 750 cm^{-1}), where tellurium atoms are threefold coordinated by oxygen atoms. As for Raman investigations, these results confirm the progressive change in the Te coordination from 4, as in αTeO_2, to 3 as in $BaTeO_3$.

On the other hand, the shape of the $(1-x)TeO_2 + xTiO_2$ glass spectra, Fig. 11, is rather similar for the whole glassy range ($0 \leq x \leq 0.3$). Nevertheless, if no drastic change is observed for the shoulder at 760 cm^{-1}, the large absorption band centered at 640 cm^{-1} is splitted into two components at 615 and 670 cm^{-1} for $x = 0.30$. Similar absorption bands are recorded for the crystallized compound $TiTe_3O_8$ close to the glass composition $x = 0.25$. Thus, both tellurium and titanium atoms must exhibit the same coordination in glassy and crystalline states: 4 and 6, respectively.

Moreover, in the $0.8TeO_2 + xTiO_2 + (0.2-x)BaO$ glasses (Fig. 12), it can be observed a progressive change in

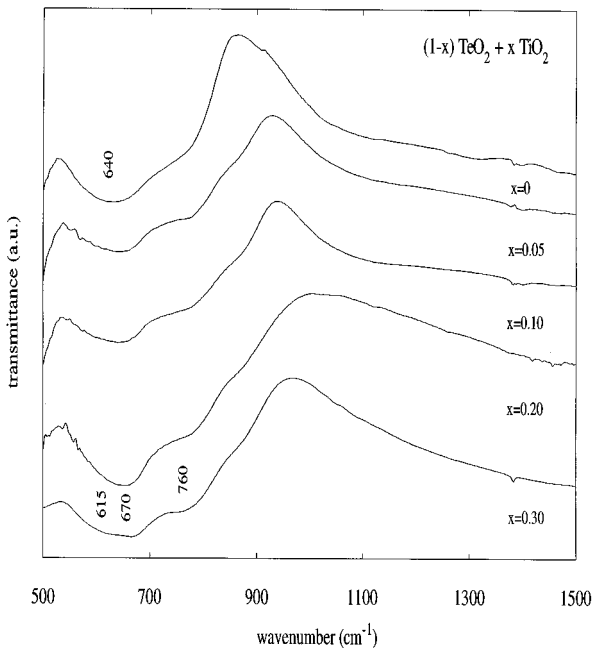

FIG. 11. Infrared spectra of the $(1 - x)TeO_2 + xTiO_2$ glasses.

the coordination of Te atoms. For $x = 0$, the tellurium atoms have an intermediate environment called $3 + 1$, while for $x = 0.20$, the glass spectrum exhibits similarities with that of $TiTe_3O_8$.

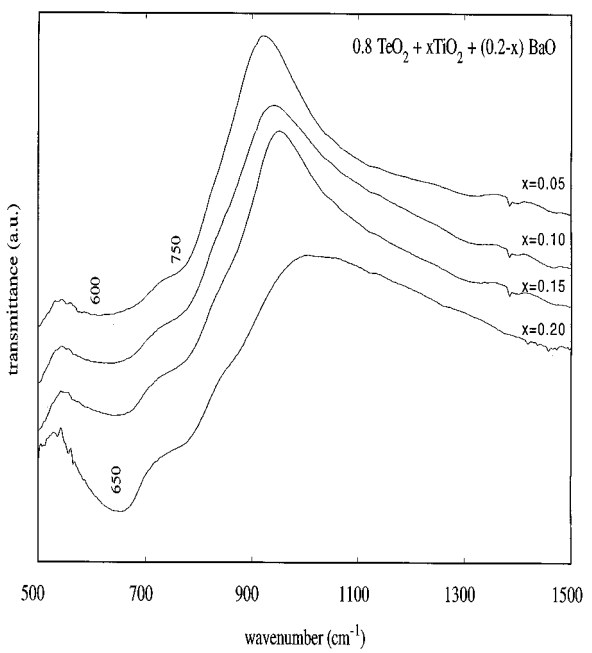

FIG. 12. Infrared spectra of the $0.8TeO_2 + (0.2 - x)BaO + xTiO_2$ glasses.

TABLE 2
Nonlinear Absorption and Refractive Indices of the BaO–TeO_2–TiO_2 Ternary Glasses

Glass composition					
BaO (%)	TeO_2 (%)	TiO_2 (%)	L_{eff} (cm)	β (cm/GW)	n_2 (10^{-18} m$^2 \cdot$ W^{-1})
7	93	0	0.175	12 ± 2	4.1 ± 0.8
10	90	0	0.189	10 ± 1	4.2 ± 0.8
15	85	0	0.179	5.6 ± 1	6.2 ± 0.8
15	85	0	0.135	5.2 ± 0.1	6.6 ± 0.5
15	85	0	0.231	5.7 ± 0.2	—
20	70	10	0.175	7.8 ± 0.7	5.8 ± 0.9
15	80	5	0.170	9.6 ± 0.4	3.3 ± 0.7
10	80	10	0.173	12.6 ± 0.5	3.6 ± 0.7
10	80	10	0.161	11.5 ± 0.9	—
5	80	15	0.175	14 ± 0.4	—
5	90	5	0.176	9.3 ± 0.3	—
5	90	5	0.176	10.5 ± 1.4	—
0	90	10	0.178	16.3 ± 0.94	—
0	90	10	0.171	15.7 ± 2.7	—

Note. Some nonlinear refractive indices have not been measured because of the optical scattering. The uncertainties are essentially due to the uncertainty on the n_2 (CS_2) value.

NONLINEAR OPTICAL CHARACTERIZATIONS

The most representative results of both nonlinear absorption (β) and refractive index (n_2) obtained for glasses synthesized in the TeO_2–BaO–TiO_2 system are gathered in Table 2. The highest experimental β value is obtained for the $0.9TeO_2 + 0.1TiO_2$ composition while the $0.85TeO_2 + 0.15TiO_2$ glass has the lowest but the largest n_2 index (6.6×10^{-18} m^2/W). This exceptional non-linear coefficient is about 10 times larger than that of TiO_2-containing phosphate or borophosphate glasses (25) or that of several glassy systems such as PbO–TiO_2–SiO_2–K_2O (26) and 3 times larger than some tellurium oxide glasses (23, 27). It is obvious from Table 2 that the TiO_2 insertion into the TeO_2-based glasses has an important influence on the nonlinear absorption and that n_2 varies with the BaO content, not with the TiO_2 content.

DISCUSSION

Infrared and Raman spectroscopies make it possible to determine whether a TeO_2-based glass is built up of TeO_4 or TeO_3 groups according to their vibration modes. In this paper, we have studied the structural evolution of the glassy network with the modifier content by comparing the positions of the absorption (IR) and diffusion (Raman) bands with those of crystalline compounds of well-known structure. The typical broadening of the vibration bands due to the glassy state has been observed for all the spectra. These latter often present similarities with the spectra of the

corresponding crystalline phase, which is directly due to their common vibration units.

Both Raman and infrared spectroscopies lead to the same conclusion:

— Pure TeO_2 glass is built up from TeO_4 units as in αTeO_2, but they are more distorted in the glassy state than in the crystalline state.

— For the $(1-x)TeO_2 + xBaO$ pseudo binary system, if the characteristic absorption bands of Ba–O bonds cannot be observed (less than 400 cm^{-1}), the coordination of tellurium atoms is well determined: it decreases progressively from 4 ($x = 0$) to 3 ($x = 0.4$) through the so-called $3 + 1$ coordination. When the modifier content increases, there is a continuous and progressive deformation of the Te environment with a shortening of one of the two axial bonds and, conversely, a lengthtening of the other. Furthermore, for high BaO content ($x \geq 0.20$), nonbridging oxygen atoms are present.

— The tellurium atom surroundings are quite different when the added modifier is TiO_2. In this case, the fourfold coordination remains the same for the whole glassy range, but the distortion seems to be slightly more pronounced. On the other hand, the titanium atoms possess the distorted octahedral coordination as encountered in TiO_2 rutile or $TiTe_3O_8$. Nonbridging oxygen atoms have not been evidenced in this pseudo binary TeO_2–TiO_2 system.

— For the pseudo ternary system, we observe a progressive coordination change of the Te atoms (3 to 4) when Ti atoms replace Ba atoms.

This different behavior of the tellurium atoms between the two pseudo binary system could be explained by their ionic/covalent character. From Pauling's electronegativity (0.9 for Ba, 1.5 for Ti, and 3.5 for O), the Ba–O bond has a stronger ionic character than that of Ti–O. The increase of Ba^{++} content favors the ionic character of these glasses, whith ninefold coordinated barium atoms as in $BaTeO_3$ (16). On the other hand, the covalent character of TiO_2 favors a tridimensional covalent network, where each atom keeps its own coordination.

The registered evolutions of the nonlinear optical properties of these studied glasses are certainly caused by the structural changes induced in the glass network by the modifier cations. The increase of n_2 with the BaO content may indicate that the glass network composed of TeO_3 tp's with nonbridging oxygen atoms is responsible for the high nonlinearities in these materials. This correlation is consistent with the theory proposed by Adair *et al.* (28) who report an increase of n_2 with the formation of nonbridging oxygen bonds if no polarizable modifying ions are present in the glass. Indeed, for bridging oxygen atoms, the two covalent bonds (Te–O–Te) serve to decrease the polarizability of the oxygen ions and, thus, the nonlinear refractive index.

Nevertheless, Ti^{4+} ions do not induce the formation of NBO. Introduction of this intermediate modifying ion into the TeO_2 glass network gives rise to increase the nonlinear optical absorption, which is mainly attributed to polarizable modifying ions rather than the NBO content.

Calculations have shown that the largest nonlinear responses are generated by the highest valency metal cations or by the maximum p–d orbital overlap (31). Thus, ions with empty or unfilled d shells such as Ti^{4+} contribute more strongly to the nonlinear polarizabilities. Further, according to Lines (31), the "d-orbitals" contributions to nonlinear polarizability are found to be negligible for bond lengths $d \geq 2.3$ Å but to increase rapidly with decreasing bond length when $d \leq 2$ Å ($d_{Ti-O} = 1.96$ Å and $d_{Ba-O} = 2.76$ Å).

In the same way, TeO_2-based glasses have a lone pair electron localized in the third equatorial direction of the Te atom, and the relatively deformability of this pair could result in a large nonlinear value.

CONCLUSION

IR and Raman spectroscopies have been used in order to approach the structure of TeO_2–BaO–TiO_2 glasses.

In the BaO–TeO_2 glassy system, the tellurium atom coordination changes, with the BaO content, from TeO_4 through TeO_{3+1} to TeO_3 with NBO. Also, the structure is depolymerized.

On the other hand, the addition of TiO_2 leads to the formation of more covalent bonds and favors a continuous network. The structural units for these glasses are distorted TiO_6 and TeO_4 polyhedra.

The highest value of β (16.3 $cm \cdot GW^{-1}$), obtained for the $0.9TeO_2 + 0.1TiO_2$ glass, may be explained by the hyperpolarization of the transition ion and the influence of the electronic lone pair of tellurium.

REFERENCES

1. J. E. Stanworth, *J. Soc. Glass Tech.* **36,** 217 (1952).
2. T. Yoko, K. Kamiya, H. Yamoda, and K. Tonaka, *J. Am. Ceram. Soc.* **71,** 70 (1988).
3. S. Noev, V. Kozhukharov, I. Gerasimova, and M. Marinov, *J. Mater. Sci.* **15,** 1153 (1980).
4. H. Nasu, T. Uchigaki, K. Kamiya, and H. Kanbara, *Jpn. J. Appl. Phys.* **31,** 3899 (1992).
5. T. Sekiya, N. Mochida, and A. Ohtsuka, *J. Non-Cryst. Solids* **168,** 106 (1994).
6. H. Nasu, O. Matsuoka, K. Kamiya, H. Kobayashi, and K. Kubodera, *J. Non Cryst. Solids* **124,** 275 (1990).
7. M. Vogel, M. J. Weber, and D. M. Krol, *Phys. Chem. Glasses* **32** (6), 231 (1991).
8. M. Sheik-Bahae, *IEEE J. Quantum Electron.* **QE-26** (4), 759 (1990).
9. N. Mochida, K. Takaoshi, K. Nakada, and S. Shibusawa, *Yogyo Kyokai Shi* **86,** 316 (1978).
10. S. Noev, V. Kozhukharov, I. Gerasimova, and B. Sidzhimov, *J. Phys. C Solid State Phys.* **12,** 2475 (1979).
11. T. Yoko, H. Yamado, and K. Tanaka, *J. Am. Ceram. Soc.* **71,** 250 (1988).

12. M. Sheik-Bahae, A. A. Said, and E. W. Van Stryland, *Opt. Lett.* **14,** 955 (1989).
13. M. Sheik-Bahae, A. A. Said, T-H. Wei, D. J. Hagan, and E. W. Van stryland, *IEEE J. Quantum Electron.* **QE-26,** 760 (1990).
14. O. Lindqvist, *Acta Chem. Scand.* **22,** 977 (1968).
15. T. Sekiya, N. Mochida, A. Ohtsuka and M. Tonokawa, *Nippon Seramikkusu Kyokai Gakujutsu Ronbunshi*, **97** (12), 1435 (1989).
16. F. Folger, Z. *Anorg. Allg. Chem.* **411,** 111 (1971).
17. K. Burdett, T. Hughbanks, J. Muller, W. Richardson, and V. Smith, *J. Am. Chem. Soc.* **109,** 3639 (1987).
18. J. A. Bland, *Acta Crystallogr.* **14,** 875 (1961).
19. F. Gonzales-Vilchez and W. P. Griffith, JCS Dalton, 1416 (1972).
20. F. Wijzen, A. Rulmont, and P. Tarte, *Spectrochim. Acta* **50** (4), 677 (1994).
21. G. Meunier and J. Galy, *Acta Crystallogr. Sect. B* **27,** 602 (1971).
22. E. Fargin, A. Berthereau, T. Cardinal, G. Le Flem, L. Ducasse, L. Canioni, P. Segonds, L. Sarger, and A. Ducasse, *J. Non-Cryst. Solids* **203,** 96 (1996).
23. T. Sekiya, N. Mochida, A. Ohtsuka, and M. Tonokawa, *J. Non-Cryst. Solids* **144,** 128 (1994).
24. Y. Dimitriev, V. Dimitrov, and M. Arnaudov, *J. Mater. Sci.* **18,** 1353 (1983).
25. S. Le Boiteux, P. Segonds, L. Canioni, L. Sarger, T. Cardinal, C. Duchesne, E. Fargin, and G. Le Flem, *J. Appl. Phys.* **81** (3), 1481 (1997).
26. X. Zhu and Z. Meng, *J. Appl. Phys.* **75** (8), 3756 (1994).
27. A. Berthereau, Y. Le Luyer, R. Olazcuaga, G. Le Flem, M. Couzi, L. Canioni, P. Segonds, L. Sarger and A. Ducasse, *Mater. Res. Bul.* **29**(9), 933 (1994).
28. R. Adair, R. Chase, and L. L. Payne. S. A., *J. Opt. Soc. Am. B* **4,** 875 (1987).
29. E. Lines, *Phys. Rev. B* **43** (14), 11978 (1991).